DRUG DEVELOPMENT AND INDUSTRIAL PHARMACY, 19(17&18), 2473-2497 (1993)

AXIAL TO RADIAL PRESSURE TRANSMISSION OF TABLET EXCIPIENTS USING A NOVEL INSTRUMENTED DIE

Harry G. Cocolas and Nicholas G. Lordi
Pharmaceutical Compaction Research Laboratory and Information Center
College of Pharmacy, Rutgers University, Piscataway, New Jersey 08855

ABSTRACT

A die instrumented with four piezoelectric force transducers was developed for use on the Rutgers Integrated Compaction Research System. It was calibrated and characterized using high density polyethylene as the calibrating material. Results showed that the radial response measured by the four die wall transducers was dependent upon the thickness of the compact being compressed and its location within the die. These two factors were incorporated into the calibration constant which converted the die wall response from voltage units into pressure units. Sample compaction profiles showing axial to radial pressure transmission of selected materials of interest in tableting were generated using this die.

INTRODUCTION

The use of an instrumented die for the measurement of the radial stresses that occur during the compaction event has been investigated by several different authors (1-15). Many different die designs have been used, ranging from Nelson's first die (1) to the many modifications made on Windheuser's segmented die (2). For most of these

Table 1
Location of piezoelectric force transducers within the instrumented die.

Transducer #	1	2	3	4
Location around die bore (degrees)	0	60	180	240
Center line of Transducer from top of die (mm)	13.97	11.00	8.05	5.08

dies, the measurement of the radial stress is confined to a limited region of the die, somewhere near the force sensor. In this study a novel instrumented die developed for use on the *Rutgers Integrated Compaction Research System* (ICRS) was characterized and calibrated. The design of this die was such that the measurement of radial stress was not limited to a narrow region of the die. This die was then used to measure the axial to radial pressure transmission of select materials of interest.

DESIGN OF ICRS INSTRUMENTED DIE

The instrumented die (PCB Piezotronics Inc., Depew, NY. Model 112M259) developed for the ICRS (Mand Testing Machines, Stourbridge, England) was designed using a 10.3 mm F-press die and the F-press die holder from the ICRS. Four piezoelectric force transducers were located in a spiral arrangement at different heights around the die bore. The specific location of each crystal is shown in Table 1 and the transducer center line locations are shown schematically in Figure 1.

By spreading out the force transducers over the length of the die bore, measurement of the die wall stress is not confined to a narrow region, but rather to the region between the upper and lower transducer locations. Each individual transducer will measure a die wall stress within its range of measurement. Its range of measurement is determined by the surface area of the force transducer. If the surface of the compact in contact with the die wall covers more than one transducer, this range will overlap with the neighboring transducers. If the compact completely covers the transducer response area, a maximum response will be received from that transducer even if a thicker

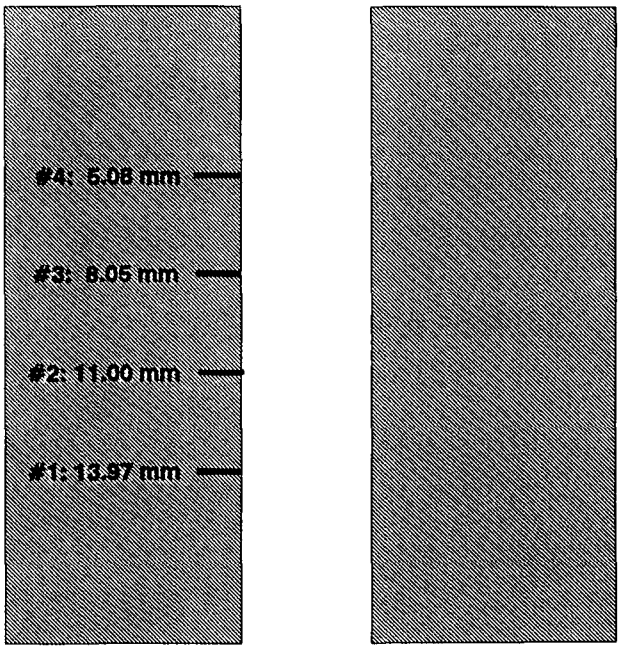

FIGURE 1
Schematic of instrumented die showing center line location of the four piezoelectric force transducers.

compact is compressed at the same location. The number of transducers responding will depend on the thickness of the compact and its location within the die bore. The responses of the individual transducers are summed to give the total die wall stress occurring within the range of the transducers responding.

Engineer's drawings (Figure 2) show the positioning of the transducers within the die and the die holder. Four holes were bored out perpendicular to the die cavity at the locations stated in Table 1. The piezoelectric transducers were placed horizontally into the holes and fixed in place. The thickness of the die wall at this point is approximately 2.54 mm. Portions of the die holder at these locations were cut away to allow for the insertion of the modified die with the transducers in place. Holes were drilled into the bottom of the die holder for the transducer leads to be routed out to connectors located on the bottom of the die holder.

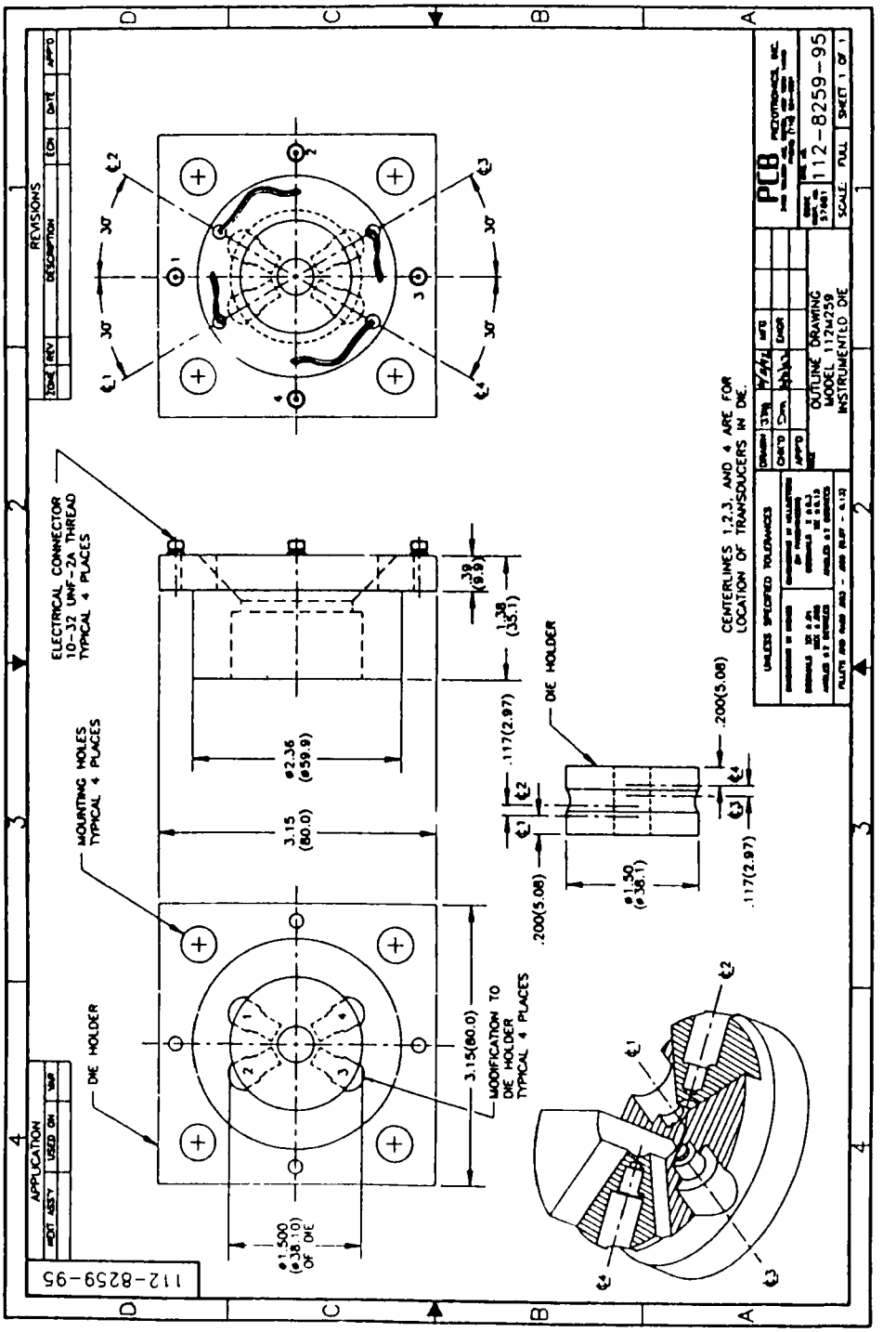

FIGURE 2
Engineer's drawings of the instrumented die.

Each transducer is connected to its own power supply (PCB Model 484M61). Voltages can either be collected individually or summed using the Summing Amplifier/Selector Switch (PCB Model 482M136). The power supplies were grounded out prior to data collection to zero the baseline before each measurement.

CALIBRATION OF ICRS INSTRUMENTED DIE

Calibration Material

High density polyethylene (HDPE) was used to calibrate the instrumented die. This material was chosen because of its ability to form a zero porosity compact under moderate pressures (ca 100 MPa). This avoids some of the problems encountered using rubber as the calibrating material as has been done in just about all previous studies.

One problem with using a rubber plug is getting it to fit perfectly inside the die cavity. Gaps between the edge of the plug and the die wall can occur from the plug being too small or the edges being cut unevenly. If the edges are uneven, there will be an uneven stress exerted on the die wall by the plug. Because of the gaps being present, the plug must expand under stress first before any contact is made with the die wall. This will create a lag time between the applied axial stress and the measured radial stress.

By using ground up rubber granules (3), this problem was avoided. However, another problem remains with rubber in that it is a porous material. In order for rubber to act as a hydraulic fluid, it should be a solid body without any pores.

The use of HDPE as a calibrating material avoids both of these problems. HDPE granules between 50 and 200 microns (Schaetti & Co., Wallisellen, Switzerland) were compressed four times under load control to 35 kN. There was no significant change in the compaction profile behavior between the third and fourth compression of the compact as shown in Figures 3 & 4. Figure 3 shows the change in compact thickness as a function of applied pressure for the first through fourth compressions. There is a large initial change in thickness during the first compression, as would be expected since the granules are being formed into a compact. Subsequent compressions caused little change in compact thickness. The change in thickness becomes linear with respect to the applied pressure once zero porosity is reached.

In Figure 4, upper punch pressure is plotted against the specific volume of the compact for the four compression cycles. Once again there is a large change during the

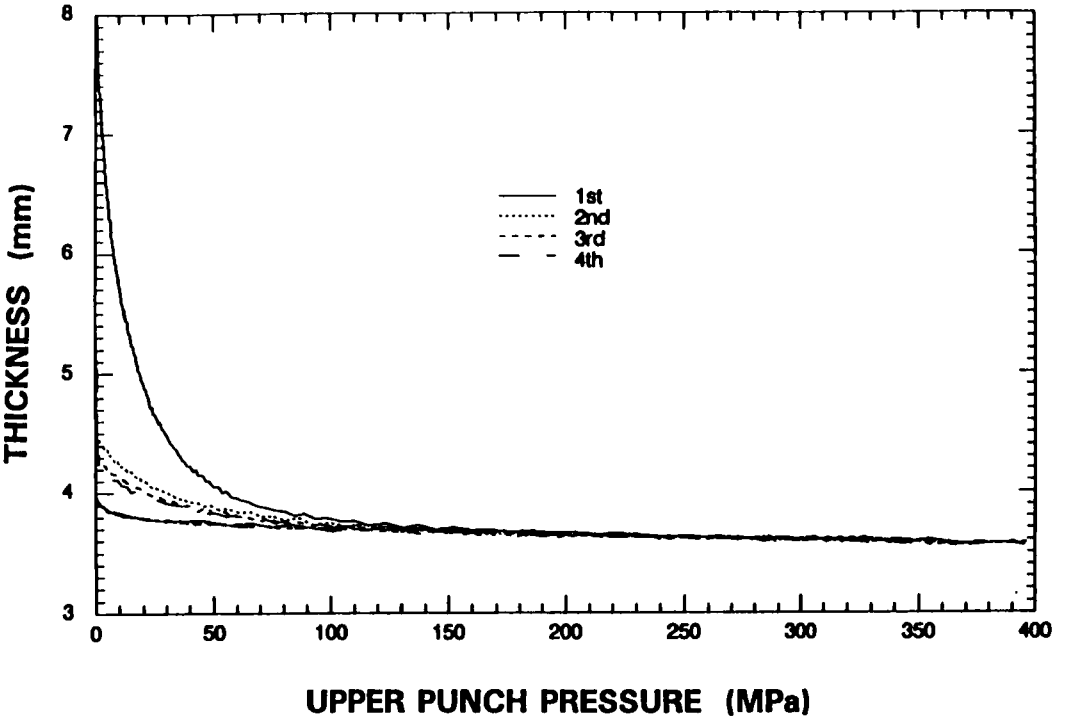

FIGURE 3
Thickness versus upper punch pressure for HDPE. 1st through 4th compression.

first compression as the compact is formed. The material behaves elastically after a zero porosity compact is formed as is evident by the almost full recovery of the volume above an applied pressure of 100 MPa

By the fourth compression the compact will reach zero porosity at a low axial pressure. Once zero porosity has been reached, the compact should approximate hydraulic behavior. There is no lag time between the applied axial pressure and the measured radial response because the compact has been formed within the die so there are no gaps between the edge of the compact and the die wall.

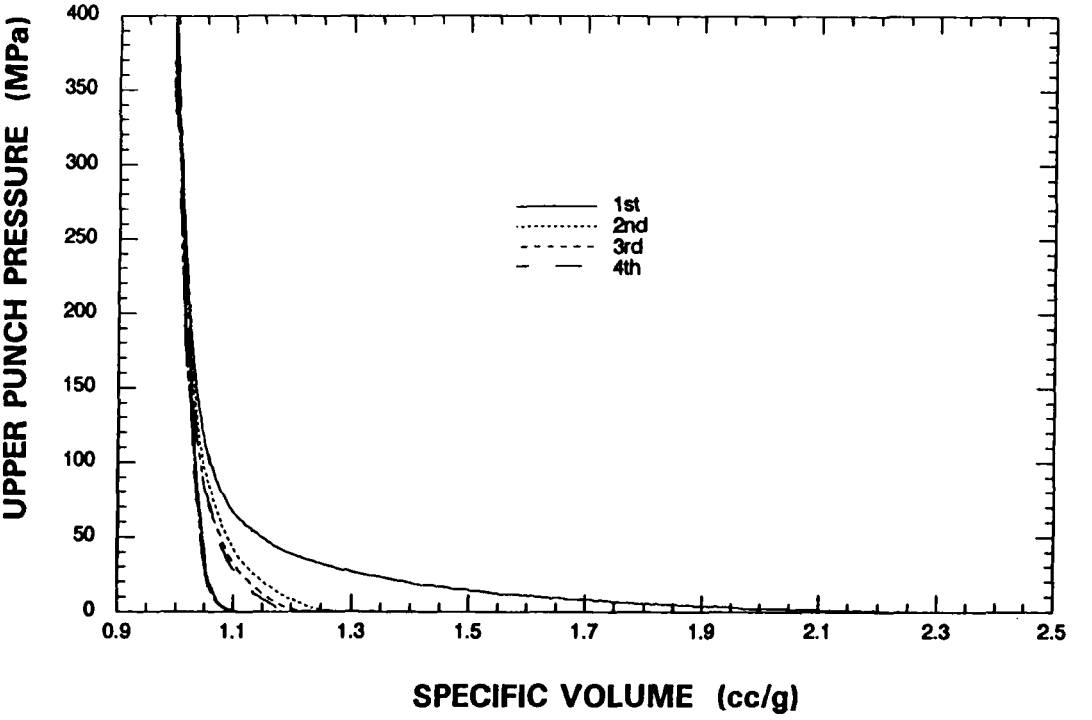

FIGURE 4
Upper punch pressure versus specific volume for HDPE. 1st through 4th compression.

Data Collection

The upper and lower punch force and their displacement were collected using a digital oscilloscope (Nicolet Model 440). The channel assignments for the Nicolet oscilloscope are listed in Table 2. Since the Nicolet only had four channels which were occupied by collecting data from the upper and lower punches, the responses from the four transducers located in the die were collected using the software package Atlantis (Lakeshore Technologies, Inc., Chicago, IL, Version 3.0) which was installed in a personal computer (PS/2 Model 25, IBM Corporation, Armonk, NY). Table 2 also shows the channel assignments for Atlantis. The upper punch force and position were also recorded by Atlantis so as to enable the data collected with Atlantis to be synchronized

Table 2
Channel assignments for data collection using Nicolet Digital Oscilloscope and the Atlantis program during die calibration experiments.

NICOLET		ATLANTIS	
Channel	**Description**	**Channel**	**Description**
1	Upper Punch Displacement	1	Upper Punch Force
2	Upper Punch Force	2	Upper Punch Displacement
3	Lower Punch Displacement	3	Die Transducer 1
4	Lower Punch Force	4	Die Transducer 2
		5	Die Transducer 3
		6	Die Transducer 4

with the data collected using the Nicolet. The two files were synchronized in time by matching the upper punch peak force.

Calibration Procedure

The summed die wall response is dependent upon the location of the compact within the die and the surface area of the compact in contact with the die wall as stated above. The two factors controlled during the calibration experiments were the location of the lower punch, and the compact thickness which is related to the surface area in contact with the die wall.

The location of the lower punch was varied by 1 mm intervals starting from a low point of 16 mm from the top of the die up to 9 mm. At 16 mm the lower punch will be below the lowest transducer whose center line is located at 13.97 mm. Above 9 mm uncompressed HDPE was too bulky to fit into the die cavity. Also, tablet compaction with the lower punch starting above this point rarely occurs.

At each lower punch starting point the thickness of the compact was varied by changing the weight of the compact. The weights were selected to roughly give compact heights ranging from approximately 1 to 6 mm in 1 mm intervals.

The material was compressed four times to 35 kN in each case. The data used for calibration of the die was only taken on the fourth compression due to reasons stated above. The waveform used for this compression cycle is shown in Figure 5. A load was applied by the upper punch and increased from 0.25 to 35 kN over 350 msec. This translates to a rate of approximately 100 kN/sec.

There is a sudden increase in the load at the beginning of the cycle due to the software control of the waveform. The upper punch must start its travel above the compact. When the cycle is initiated, the punch is commanded to seek a load of 0.25 kN. This results in a sudden jump in load followed by a constant increase up to 35 kN. The lower punch was held constant during the entire compression cycle. During each compression cycle both the upper and the lower punch forces and their displacements were measured along with the individual transducer responses.

The transmitted force as measured by the lower punch is also shown in Figure 5. If HDPE were to act purely as a hydraulic material, the lower punch force would be superimposed on the upper punch force. However, there is a small deviation indicating a departure from hydraulic behavior. This deviation is not considered to be significant and is ignored.

Compacts of selected height and lower punch starting points were also compacted using a single ended waveform under position control moving at 50 mm/sec. The upper punch starting position was varied to give compacts with differing maximum pressure and compact thicknesses. Data for these runs were also collected during the fourth compression. An advantage of using a position controlled waveform is the continuous application of pressure from the starting point without the sudden jump as seen with the load controlled waveform.

Calibration Results

The die wall responses for the individual transducers and their summed value are plotted against pressure in Figure 6. In this example the compact thickness at maximum pressure was approximately 3 mm and the lower punch starting position was 12 mm. At

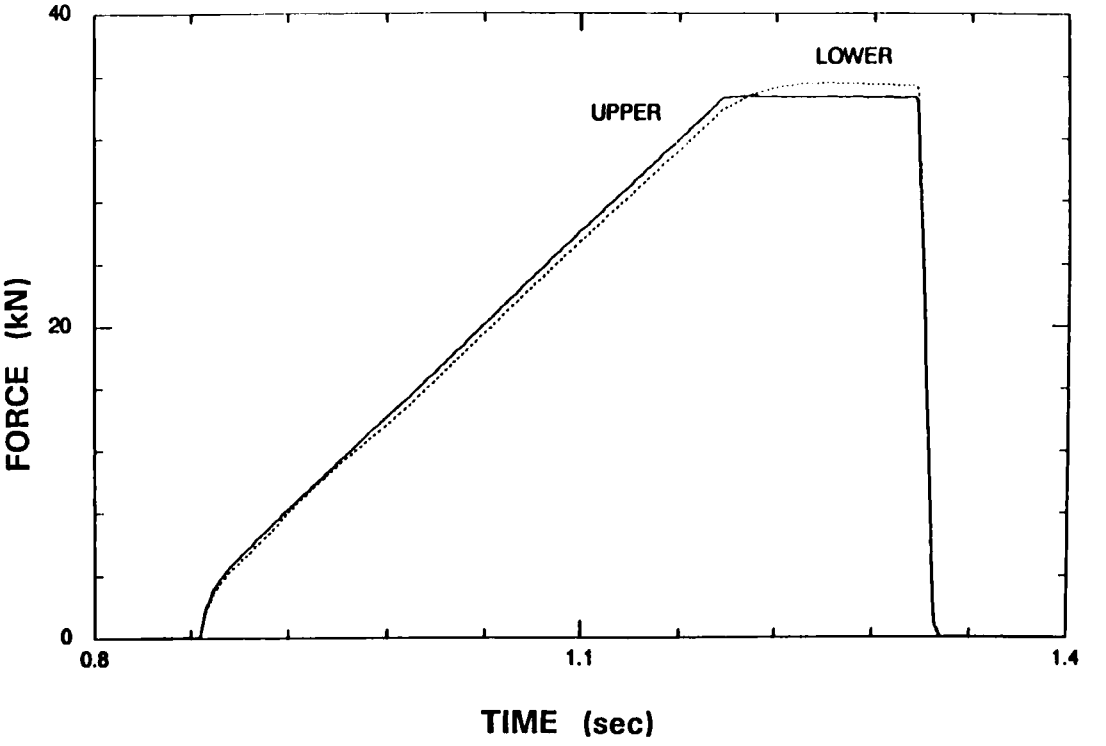

FIGURE 5
Force-time profile used for die calibration. Upper punch pressure applied under load control from 0 to 35 kN. Lower force shown is the measured response.

some point starting below 100 MPa a linear relationship between pressure and the summed die wall response begins and continues until the maximum pressure is reached. The negative response from transducer 4 is most likely due to the flexing inward of the die wall under pressure. Transducer 4 is furthest away from the point of compact contact. As the compact thickness increases and/or as the pressure decreases, this negative response diminishes.

The effect of changing compact thickness on the die wall response is shown in Figure 7. Compacts of varying thickness were all compressed at a lower punch starting point of 12 mm. As the compact thickness increases more of the compact is in contact with the transducers. Therefore, a greater response is measured. Data from the 1 mm

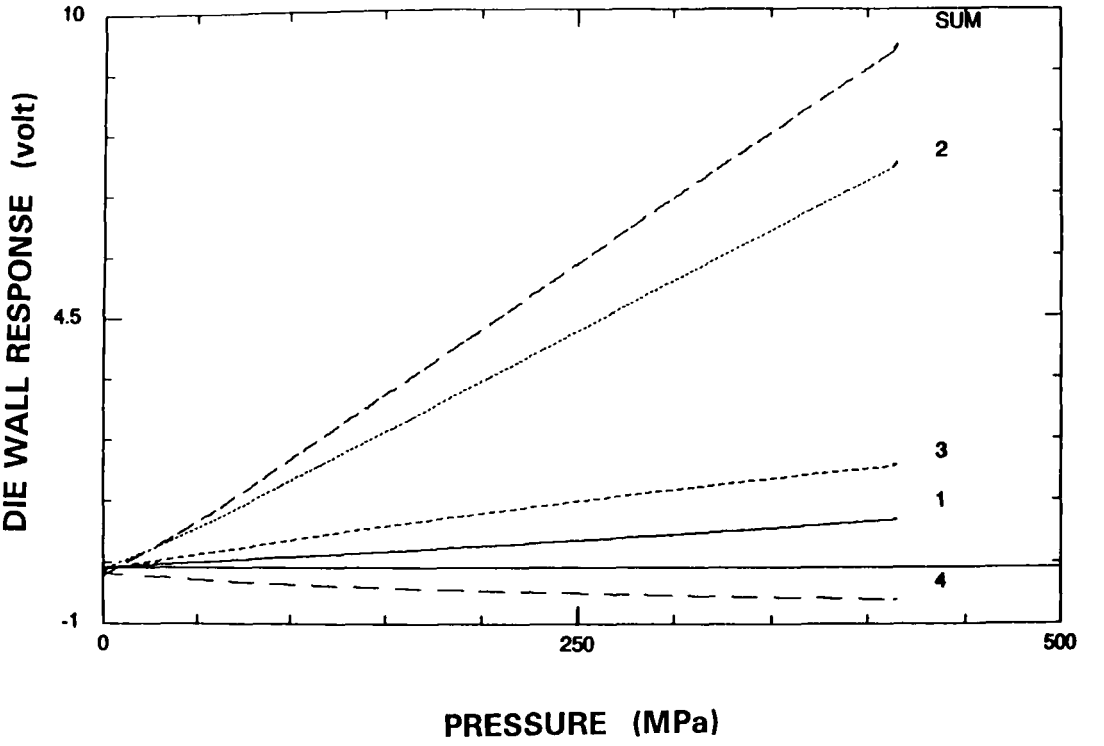

FIGURE 6
Die wall response versus upper punch pressure for HDPE with lower punch starting position = 12 mm into the die. Approximate compact thickness = 3 mm. Individual as well as summed transducer response shown.

compacts were omitted due to irregularities in the data. Compacts of this size are not normally compressed, so these data would not have much practical value.

If the summed response is normalized for the thickness of the compact, all lines should collapse into one line to give a master curve for this particular lower punch starting position. This is a variation of the work done by Holzer and Sjogren (3) in which they used the area in contact with the die wall to normalize the data.

The slope of this line gives the relationship between applied pressure and the summed response normalized for thickness. This is shown in Figure 8. Here the summed

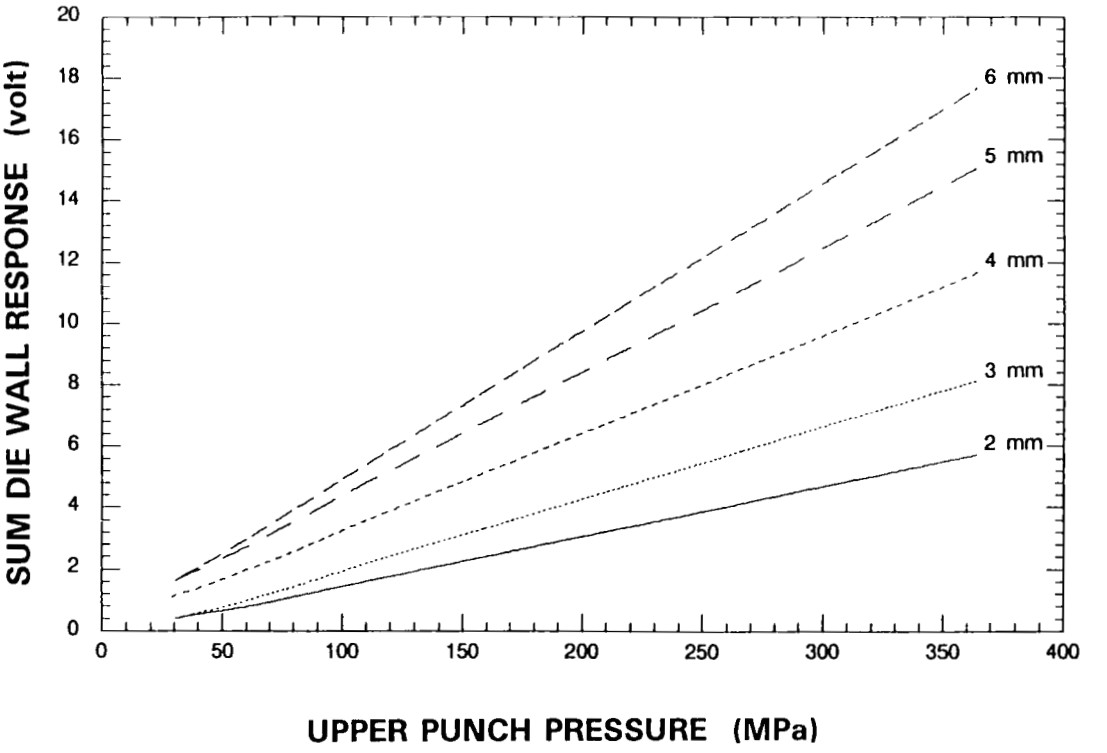

FIGURE 7
Summed die wall response versus upper punch pressure for HDPE compacts of varying thickness at a constant lower punch starting position = 12 mm into die.

die wall response divided by the thickness of the compact is plotted against the applied pressure at a lower punch starting position of 11 mm. Only the die wall response between 100 and 400 MPa was used because this was the linear region. There is some scatter in the lines due to the varying y-intercept. These intercepts can be ignored because at zero pressure there should be no die wall response. The non-zero intercepts are due to the residual pressure from the previous compression cycle and to the sudden jump in pressure observed at the beginning of the compaction cycle as described previously.

Each different starting position for the lower punch will give a master curve with a different slope as seen in Figure 9. This is because the compact is in contact with

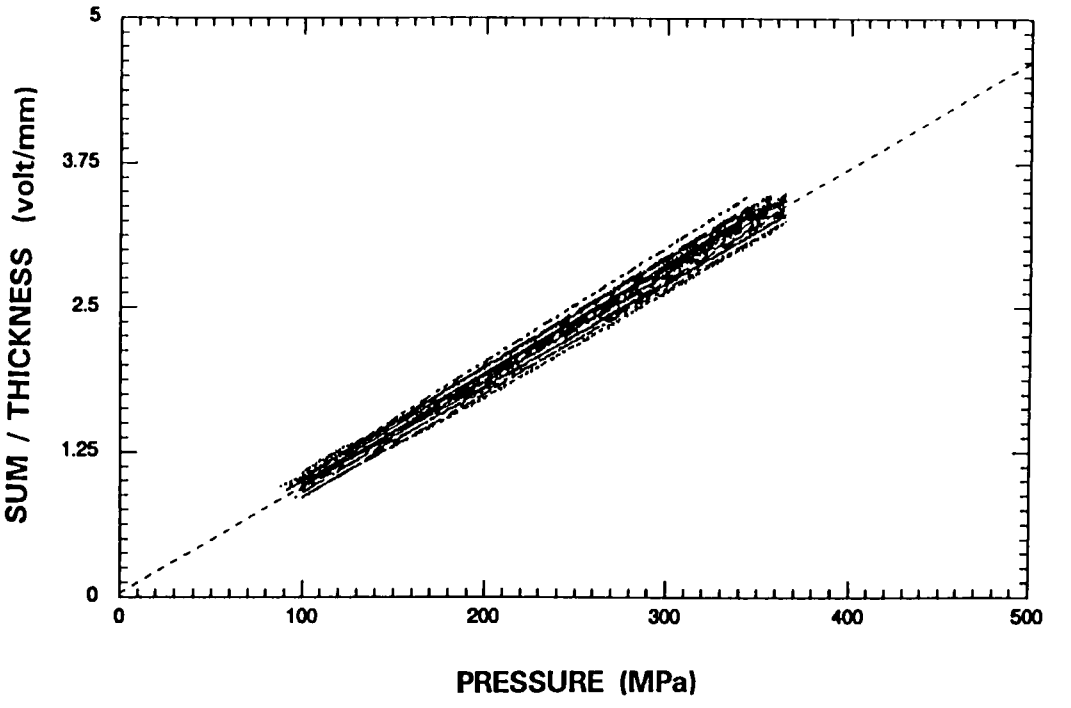

FIGURE 8
Master curve for lower punch starting position = 11 mm into die. The average slope is the dashed line passing through the origin.

different areas of the transducer at each position. In Figure 10 the master curve slopes are plotted against lower punch starting position. A maximum slope occurs at a lower punch position of 10 mm which is in the center of the die and falls off as the compact location moves toward either edge. There is a linear region between 11 and 15 mm. The master curve in this region follows Equation 1.

$$MS_L = -0.00056 \cdot LPSt + 0.0154 \quad (1)$$

ML_L = *Master slope of linear region*
LPSt = *Lower punch starting position (mm)*

The values for the master curve at each different starting position are shown in Table 3.

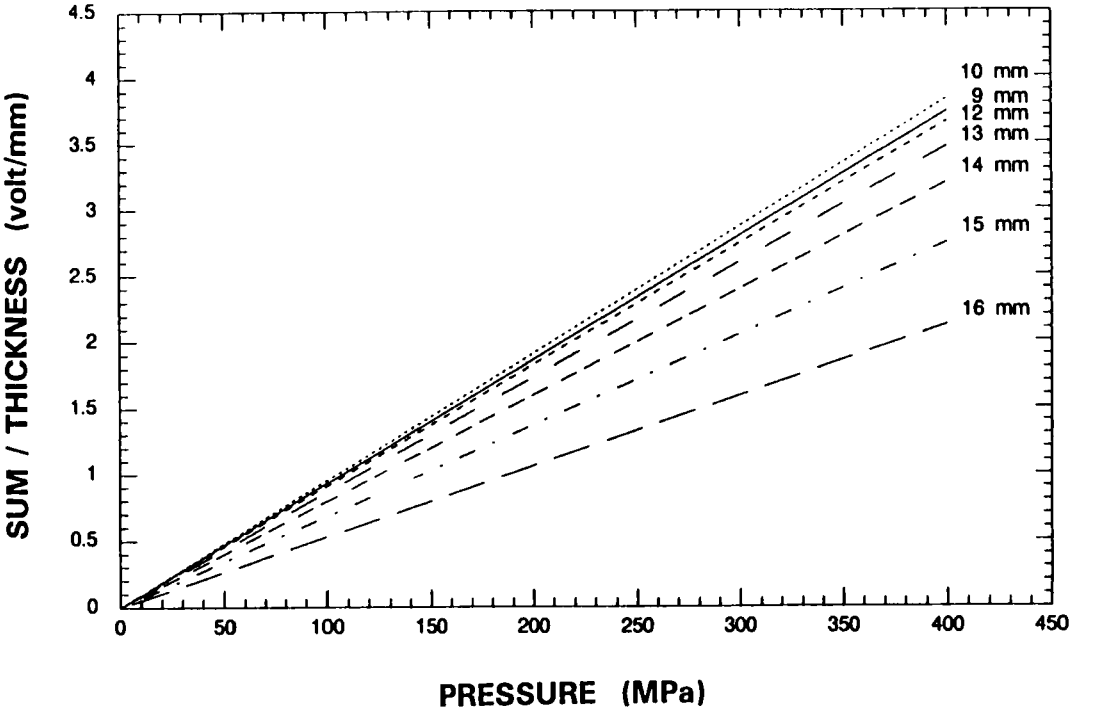

FIGURE 9
Master curves for HDPE at varying lower punch starting positions.

A test of the calibration was to conduct the same set of experiments using a position controlled waveform. This would be closer to the actual movement of a tablet press. Figure 11 shows the regression of the summed die wall response/thickness vs lower punch pressure at a lower punch starting position of 12 mm. The waveform was single-ended with the punch moving at 50 mm/sec. Each line is the fourth compression of a HDPE compact. The compact weight varied to give compacts of different thickness and maximum pressures. The average slope of the regression lines for both compression and decompression is 0.00854. This falls within the range of error of the slopes calculated using the load controlled waveforms. The similar results obtained using either load control or position control of the waveforms will enable the calibration of the die to be conducted using either method.

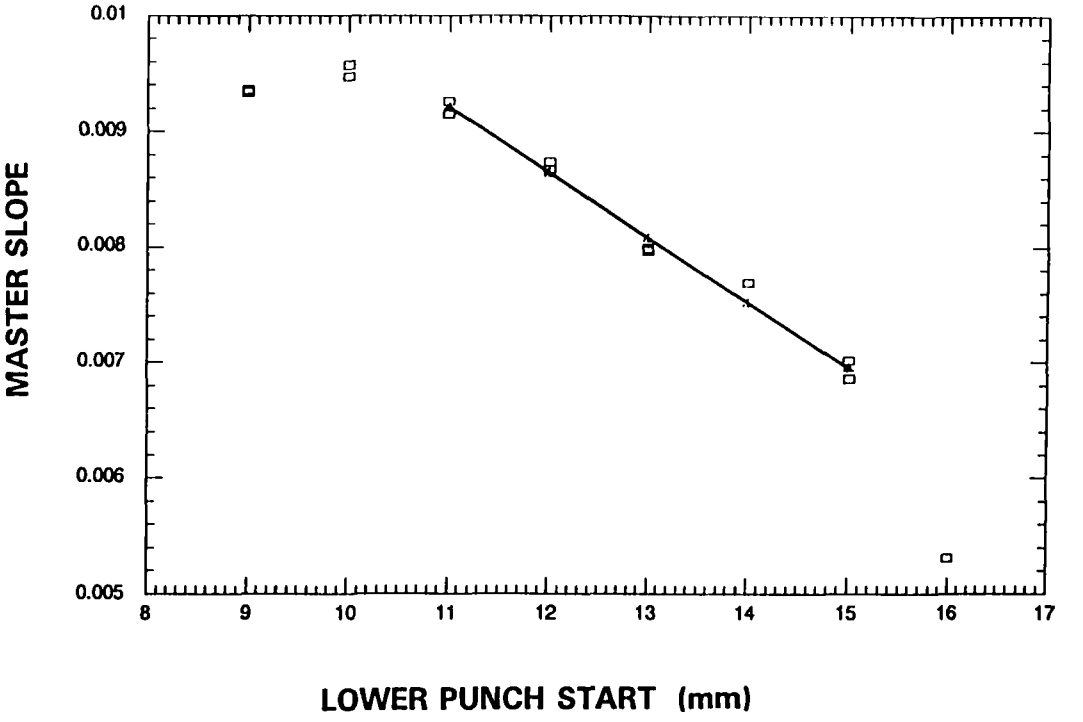

FIGURE 10

Master slope versus lower punch starting position. Best fit through linear portion of curve between 11 and 15 mm into die is shown.

Table 3

Master curve slopes and standard deviations at varying lower punch starting positions.

Lower Punch Starting Position (mm)	Master Slope	Standard Deviation
9	0.00937	0.0005
10	0.00956	0.0004
11	0.00929	0.0003
12	0.00877	0.0003
13	0.00804	0.0003
14	0.00776	0.0003
15	0.00696	0.0004
16	0.00534	0.0008

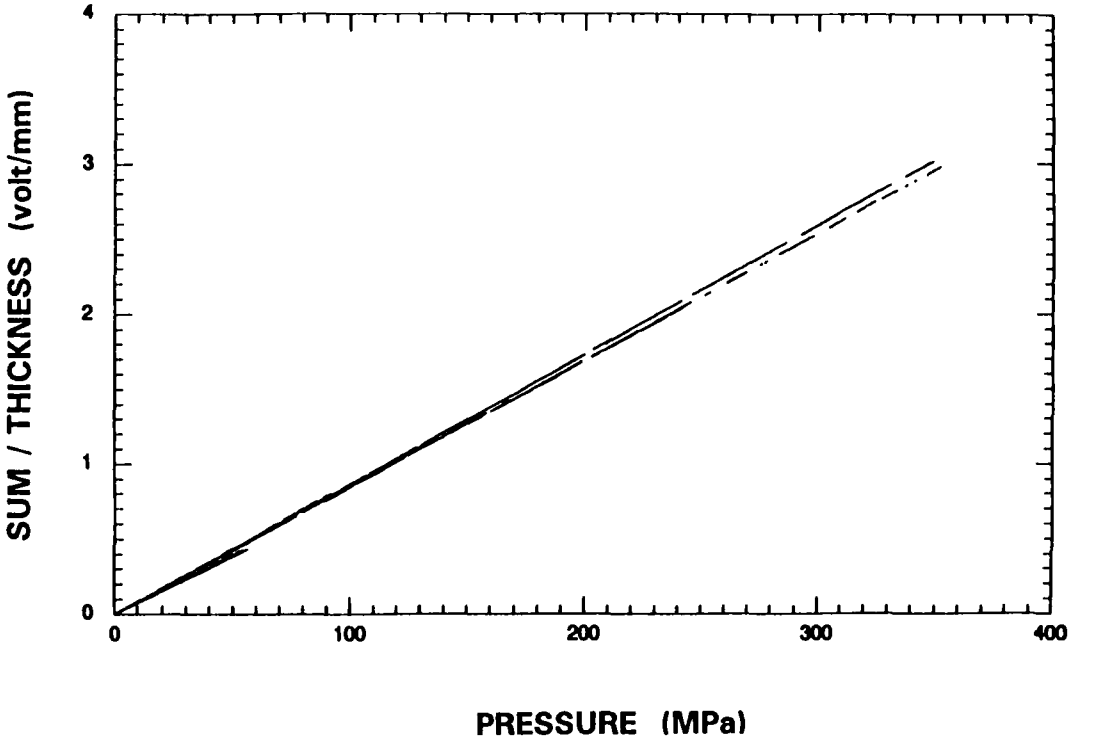

FIGURE 11
Regression of Summed DWR/Thickness versus lower punch pressure for HDPE compacts compressed using a single-ended profile with a punch velocity of 50 mm/sec.

COMPACTION PROFILES OF SELECTED MATERIALS

Sample compaction profiles for several materials have been generated and are displayed in Figures 12-20. Symbols represent the observed data points, while the solid lines are best fit regression lines though the linear segments. Each material was compacted in the ICRS without any lubrication. A single-ended sawtooth punch displacement profile with a punch velocity of 50 mm/sec was used for all compaction events. Poisson's ratio has been calculated for each material based on the initial slope before the yield point. Both of these values are listed in Table 4.

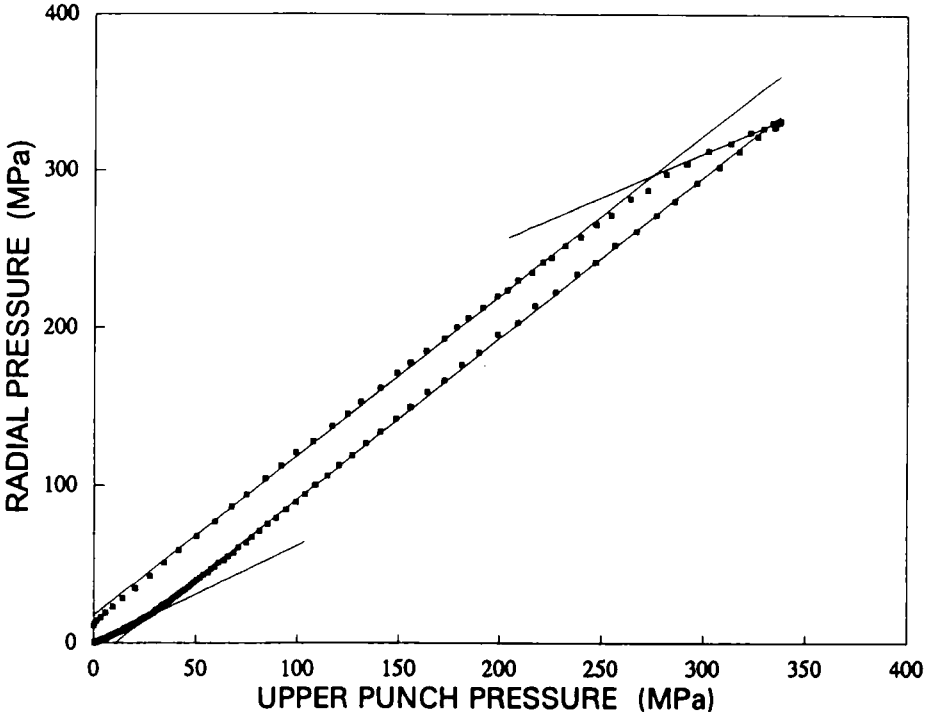

FIGURE 12
Compaction profile for High Density Polyethylene.

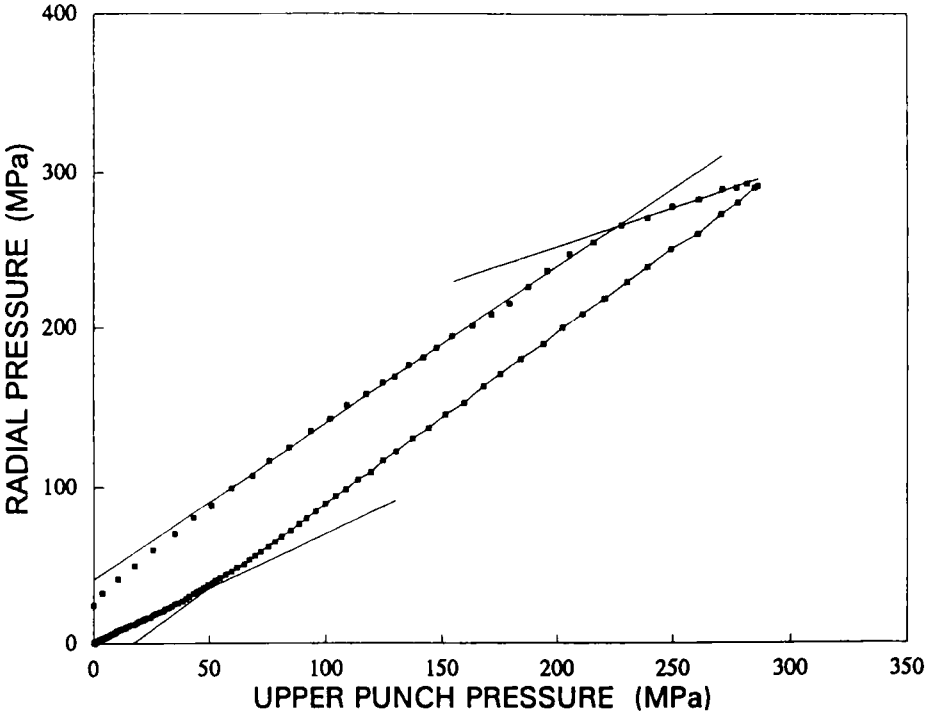

FIGURE 13
Compaction profile for Polyethylene 8000.

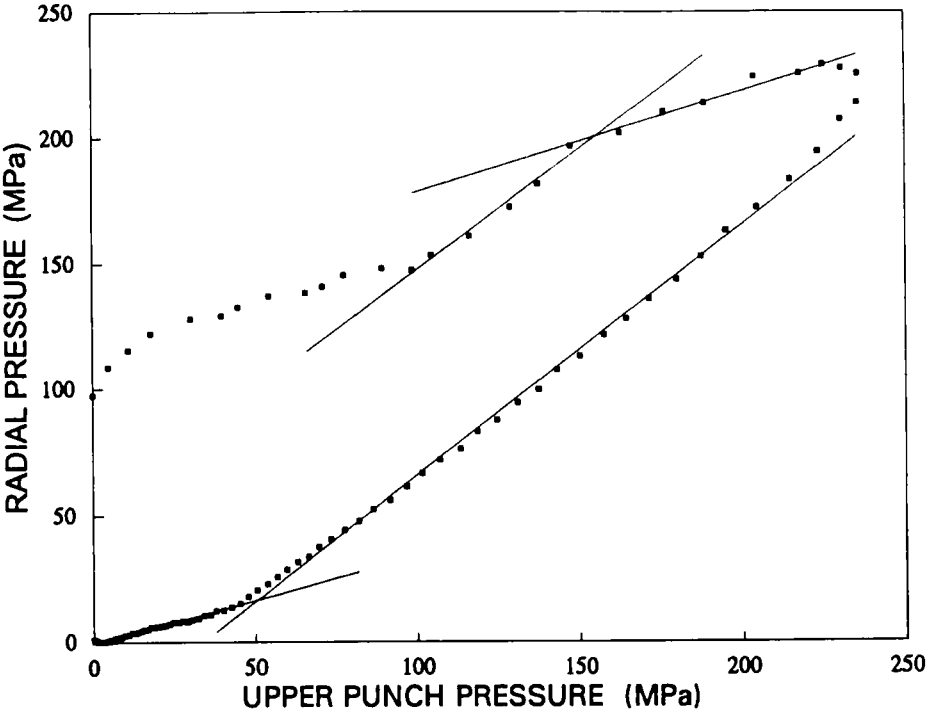

FIGURE 14
Compaction profile for Sodium Chloride.

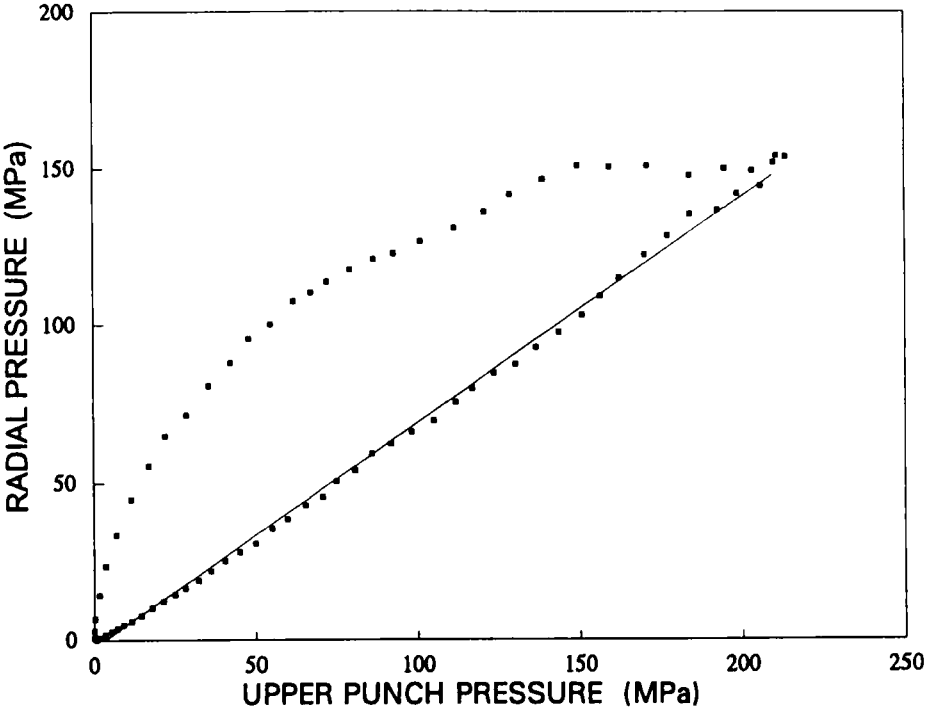

FIGURE 15
Compaction profile for 100 μm Glass Beads.

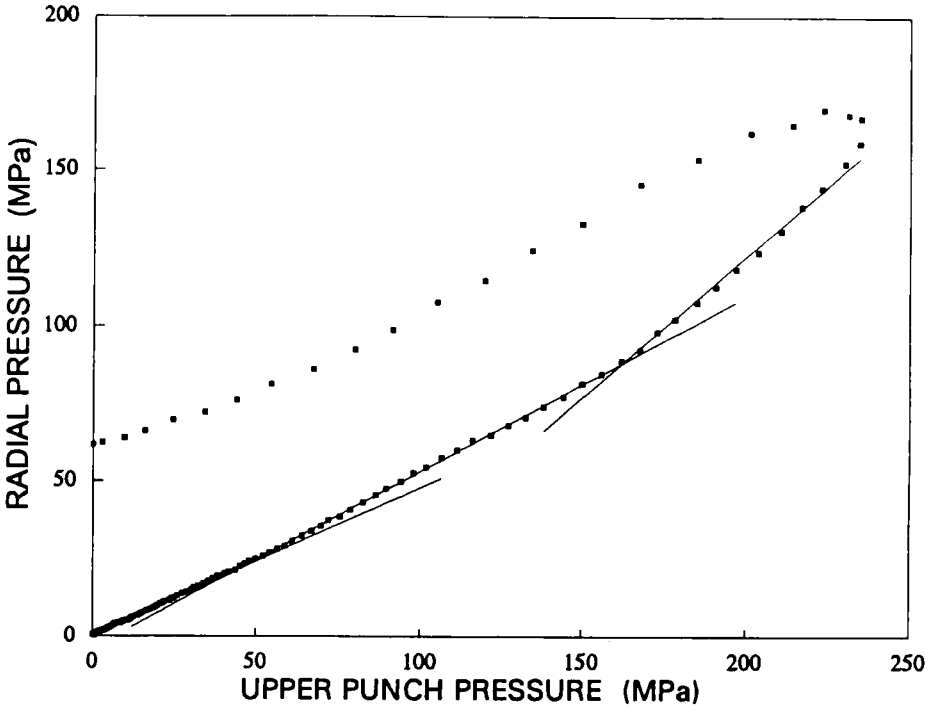

FIGURE 16
Compaction profile for Spray Dried Lactose.

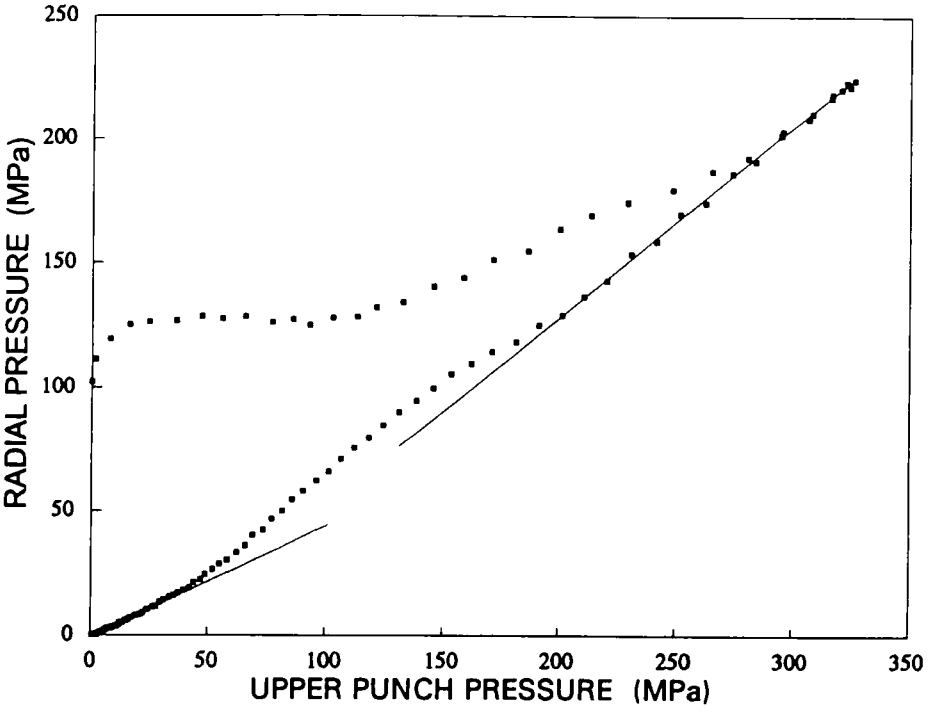

FIGURE 17
Compaction profile for Dicalcium Phosphate.

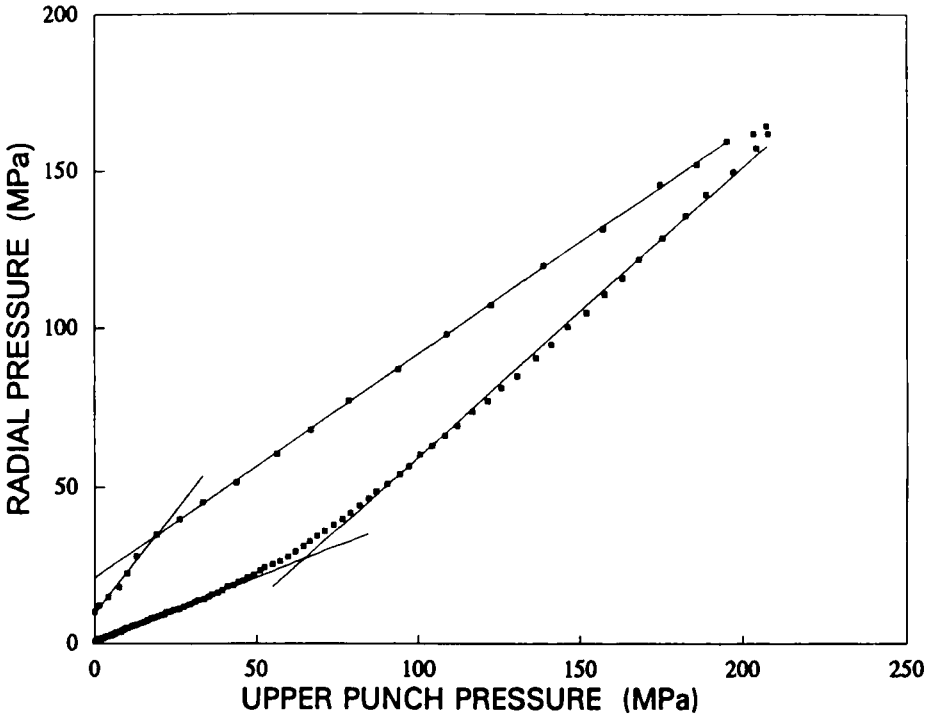

FIGURE 18
Compaction profile for Corn Starch, NF.

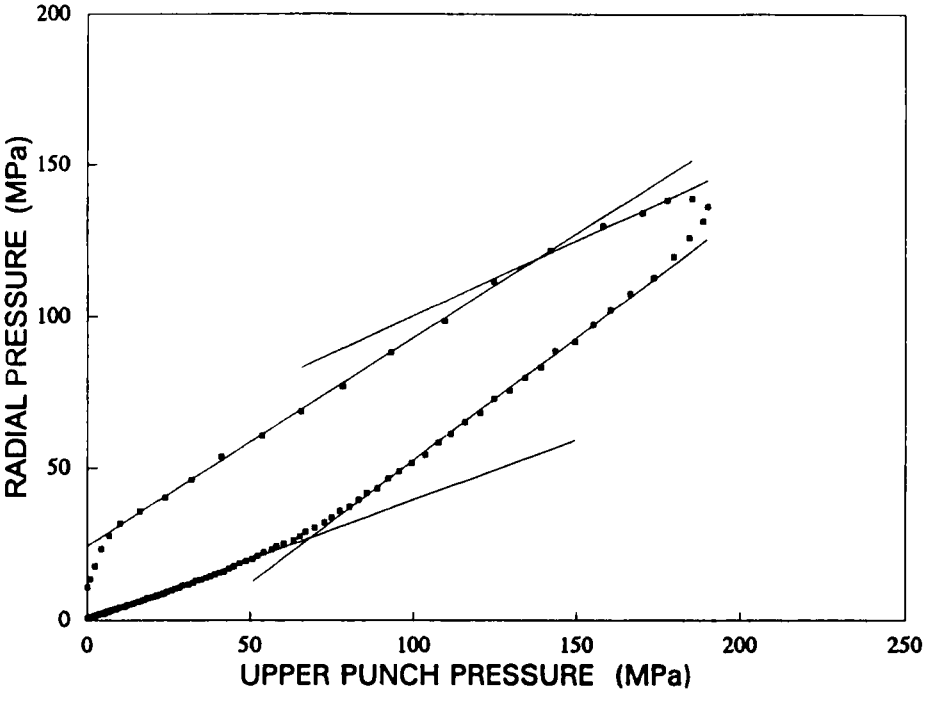

FIGURE 19
Compaction profile for Starch 1500.

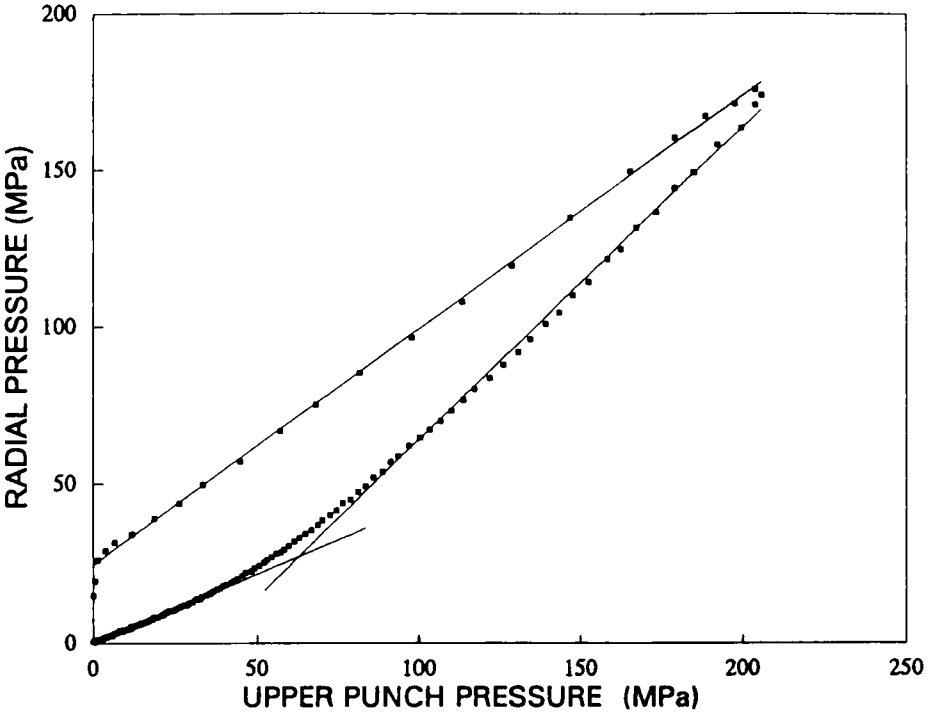

FIGURE 20
Compaction profile for National 1551.

The relationship between the initial slope and poisson's ratio is shown in Equation 2 as defined by Long (12).

$$\sigma_r = \sigma_a \cdot \left(\frac{\nu}{1 - \nu}\right) \quad (2)$$

HDPE and PEG 8000 (Union Carbide), Figures 12 and 13 respectively, showed classic compaction profiles as defined in the literature by Long (11,12) and Carstensen (16). Both of these materials followed the pattern of a material exhibiting a constant yield stress in shear after the elastic limit was reached with the slope of this segment approaching unity. During decompression elastic recovery was observed having the same slope as the initial portion of the curve. This was followed by further recovery after another yield point. Poisson's ratio of 0.38 for HDPE fell into the range of 0.320 to 0.392 reported by Vangsness (17).

Table 4
Poisson's ratio derived from the initial slope before the elastic limit using Equation 2. Terminal slope of last linear segment prior to maximum pressure.

MATERIAL	Initial Slope	ν	Terminal Slope
HDPE	0.621	0.38	1.02
PEG 8000	0.701	0.41	1.08
NaCl	0.305	0.23	1.10
Corn Starch NF	0.392	0.28	1.01
Starch 1500	0.373	0.27	1.02
National 1551	0.436	0.30	1.08
Glass Beads	0.552	0.36	0.744
Spray Dried Lactose	0.492	0.33	0.951
Dicalcium Phosphate	0.471	0.32	0.750

Not all of the compaction profiles showed ideal behavior. Krycer et al (18) point out that ideal behavior assumes a non-porous plug. Compacts involved in this study are all porous with the exception of HDPE and PEG 8000 at higher pressures. All other materials showed more than one break point as the pressure was increased. This made determination of the yield point questionable. The slope of the last linear segment prior to the maximum pressure was calculated for each material and listed in Table 4 as a reference to compare materials.

Sodium chloride (Fisher Scientific), which has been described as both a Mohr body (19) and a body with a constant yield stress in shear (10), is shown in Figure 14. Although the slope after the yield point is not constant, it appears to approach unity. This suggests that sodium chloride is behaving like a body with a constant yield stress in shear.

The compression cycle for 100 μm glass beads is shown in Figure 15. The slope after the yield point is less than unity as would be expected for a body exhibiting

behavior similar to a Mohr body. The beads deform by brittle fracture and are non-bonding as observed the inability to form an intact compact as well as the lack of any residual die wall pressure. Two other brittle fracture materials, spray dried lactose (Foremost) and dicalcium phosphate (E. Mendell Co.), are shown in Figures 16 and 17 respectively. These two materials also exhibit profiles similar to a Mohr body, with the slope after the yield point being less than unity. The profile for spray dried lactose is similar in shape to a profiles reported by Obiorah (19), while the dicalcium phosphate profile is similar to a profile reported by Krycer et al (18).

Compaction profiles for Corn Starch, NF (Amend Drug & Chemical), a partially hydrolyzed starch (Starch 1500, Colorcon), and a fully hydrolyzed starch (National 1551, National Starch) are shown in Figures 18-20. All three compaction profiles have the same general shape with a non-linear slope after the yield point which approaches unity. This would suggest that starches are behaving like a body with a constant yield stress in shear. Comparison of the three starches shows that National 1551 has a higher poisson's ratio and yield strength than Corn Starch, NF and Starch 1500. According to Obiorah (19), this is an indication that a stronger compact has been formed.

CONCLUSIONS

The summed voltage of the four individual transducers will be used in the measurement of the die wall response. This gives a much broader coverage of the response measured in the die cavity than if individual transducers had been used.

If the lower punch falls within the linear region of 11 to 15 mm into the die, then the conversion of the die wall response from volts into units of pressure will be covered by Equation 1. If the lower punch is outside of this range, then an individual master slope must be obtained for each position and applied using Equation 3.

$$DWP = \frac{\left(\frac{DWS}{THICK}\right)}{MS} \qquad (3)$$

DWP = *Die wall pressure* (*MPa*)
DWS = *Die wall signal* (*volt*)
$THICK$ = *Compact thickness* (*mm*)
MS = *Master slope* $\left(\frac{volt}{mm\text{-}MPa}\right)$

Equation 3 is a modification of the calibration equation used by Holzer and Sjogren (3) with the thickness being substituted for the area and the intercepts being ignored. Master slopes for 8, 9, 10, and 16 mm into the die have already been determined (Table 3).

It has been shown that HDPE can be used in the calibration of an instrumented die. Above 100 MPa it approximates hydraulic behavior with similar compression properties as those of rubbers and fluids.

Use of the instrumented die to generate compaction profiles for selected materials gave results that were similar to those seen in the literature. However, deviations from linearity were observed past the yield point for many materials. This could be due to a failure of the original models described by Long (11,12). His assumptions were based on a nonporous plug. With the exception of HDPE and PEG 8000 at higher pressures, none of these materials could be considered non-porous. The lack of die wall lubrication, especially with sodium chloride and the brittle fracture materials, could also have influenced the shape of the profile.

ACKNOWLEDGEMENTS

The authors would like to acknowledge ICI Pharmaceuticals Inc. for financial support through a fellowship and partial funding of the instrumented die, PCB Piezotronics, Inc. for designing, building, and partially funding the instrumented die, and Dr. Russell Somma for his ideas on this project.

REFERENCES

1. E. Nelson, J. Am. Pharm. Assn. 44, 494 (1955).
2. J. Windheuser, J. Misra, S. Eriksen, and T. Higuchi, J. Am. Pharm. Assn., 52, 767 (1963).
3. A. Holzer and J. Sjogren, Int. J. Pharm., 3, 221 (1979).
4. J. Carless and S. Leigh, J. Pharm. Pharmacol., 26, 289 (1974).
5. E. Hiestand, J. Wells, C. Peot, and J. Ochs, J. Pharm. Sci., 66, 510 (1977).
6. T. Higuchi, T. Shimamoto, S. Eriksen, and T. Yashiki, J. Pharm. Sci., 54, 111 (1965).
7. P. Huckel and M. Summers, J. Pharm. Pharmacol., 36 Supp., 6P (1984).
8. P. Huckel and M. Summers, J. Pharm. Pharmacol., 36, 722 (1985).

9. I. Krycer, D. Pope, and J. Hersey, Int. J. Pharm., 12, 113 (1982).
10. S. Leigh, J. Carless, and B. Burt, J. Pharm. Sci., 56, 888 (1967).
11. W. Long, Powder Metallurgy, 6, 73 (1960).
12. W. Long, In Special Ceramics 1962, Academic Press, London and New York, 1963, pp. 327-340.
13. B. Obiorah and E. Shotton, J. Pharm. Pharmacol., 28, 629 (1976).
14. K. Ridgway, J. Pharm. Pharmacol., 18 Supp, 176S (1966).
15. M. Summers, R. Enever, and J. Carless, J. Pharm. Pharmacol, 28, 89 (1976).
16. J.T. Carstensen, "Solid Pharmaceutics: Mechanical Properties and Rate Phenomena", Academic Press, New York, 1980.
17. T.S. Vangsness. ANTEC '92, 403 (1992).
18. I. Krycer, D. Pope, and J. Hersey, Drug Devel. Ind. Pharm., 8, 307 (1982).
19. B. Obiorah, Int. J. Pharm., 1, 249 (1978).